Deep-Sea Research I 106 (2015) 183–193

Contents lists available at ScienceDirect

Deep-Sea Research I

journal homepage: www.elsevier.com/locate/dsri

Bathymodiolus growth dynamics in relation to environmental fluctuations in vent habitats

K. Nedoncelle [a,1], F. Lartaud [a], L. Contreira Pereira [a,2], M. Yücel [a,3], A.M. Thurnherr [b], L. Mullineaux [c], N. Le Bris [a,*]

[a] Sorbonne Universités, UPMC Univ Paris 06, CNRS, Laboratoire d'Ecogéochimie des Environnements Benthiques, Observatoire Océanologique de Banyuls, F-66650 Banyuls/Mer, France
[b] Division of Ocean and Climate Physics, Lamont-Doherty Earth Observatory, Palisades 10964, New York
[c] Biology Department, Woods Hole Oceanographic Institution, Woods Hole, MA 02543, United States

ARTICLE INFO

Article history:
Received 27 May 2015
Received in revised form
14 September 2015
Accepted 5 October 2015
Available online 28 October 2015

Keywords:
Shell mineralization
Chemosynthetic ecosystem
Deep-sea environmental dynamics
Hydrothermal ecosystem
In situ monitoring
Recolonization
Disturbance
Growth rate
Vent mussels

ABSTRACT

The deep-sea mussel *Bathymodiolus thermophilus* is a dominant species in the East Pacific Rise (EPR) hydrothermal vent fields. On the EPR volcanically unstable area, this late colonizer reaches high biomass within 4–5 years on new habitats created by lava flows. The environmental conditions and growth rates characterizing the reestablishment of *B. thermophilus* populations are however largely unknown, leaving unconstrained the role of this foundation species in the ecosystem dynamics. A typical example from the vent field at 9°50'N that was affected by the last massive eruption was the Bio-9 hydrothermal vent site. Here, six years later, a large mussel population had reestablished. The von Bertalanffy growth model estimates the oldest *B. thermophilus* specimens to be 1.3 year-old in March 2012, consistent with the observation of scarce juveniles among tubeworms in 2010. Younger cohorts were also observed in 2012 but the low number of individuals, relatively to older cohorts, suggests limited survival or growth of new recruits at this site, that could reflect unsuitable habitat conditions. To further explore this asumption, we investigated the relationships between mussel growth dynamics and habitat properties. The approach combined sclerochronology analyses of daily shell growth with continuous habitat monitoring for two mussel assemblages; one from the Bio-9 new settlement and a second from the V-vent site unreached by the lava flow. At both vent sites, semi-diurnal fluctuations of abiotic conditions were recorded using sensors deployed in the mussel bed over 5 to 10 days. These data depict steep transitions from well oxygenated to oxygen-depleted conditions and from alkaline to acidic pH, combined with intermittent sulfide exposure. These semi-diurnal fluctuations exhibited marked changes in amplitude over time, exposing mussels to distinct regimes of abiotic constraints. The V-vent samples allowed growth patterns to be examined at the scale of individual life and compared to long-term records of habitat temperature and oceanographic mooring data in the years following the eruption. Both shell growth and habitat temperature at V-vent varied over the spring-neap tidal cycle and over longer periods of c.a. 60 days. The correlation of growth rate with temperature and, for some individuals, with current velocities supports the idea that tidal forcing impacts growth. Its influence on habitat conditions includes the spring-neap cycle, which is not reflected in current velocities but influences the venting rate. Additionally, it is expected that mesoscale eddies periodically passing across the ridge imprint shell growth through the influence of bottom current on the decimeter-thick mixing interface where mussels thrive. We conclude that diurnal-semidiurnal tidal fluctuations exert major abiotic constraints on *B. thermophilus* mussels and that low-frequency fluctuations act as significant determinants on growth. Finally, we postulate that the modulation of tidal fluctuations by large-scale hydrodynamic forcing ultimately constrains the capacity

* Corresponding author.
E-mail addresses: karine.nedoncelle@hotmail.fr (K. Nedoncelle), franck.lartaud@obs-banyuls.fr (F. Lartaud), leonardocontreira@gmail.com (L. Contreira Pereira), myucel@ims.metu.edu.tr (M. Yücel), ant@ldeo.columbia.edu (A.M. Thurnherr), lmullineaux@whoi.edu (L. Mullineaux), lebris@obs-banyuls.fr (N. Le Bris).
[1] Present address: IRCAN, INSERM U1081-CNRS UMR 7284 Université de Nice Sophia – Antipolis, 28, Avenue de Valombrose 06107 Nice Cedex 2, France.
[2] Present address: Laboratório de Hidroquímica-IO/FURG, Rio Grande, Brasil.
[3] Present address: Middle East Technical University, Institute of Marine Sciences, 33731 Erdemli, Mersin, Turkey.

http://dx.doi.org/10.1016/j.dsr.2015.10.003

of this mussel species to form high biomass aggregations. This study indeed shows that the absence of these strong hydrodynamic drivers would limit the alternance of oxic and sulfidic conditions and significantly affect the growth rate of this species over time.

1. Introduction

Deep-sea vent mussels of the genus *Bathymodiolus* exploit a range of chemical resources available in their habitats in the form of dissolved reduced (H_2S, CH_4, H_2) and oxidized (O_2) compounds that are used for CO_2 fixation by flexible chemoautotrophic bacterial symbioses (Le Bris and Duperron, 2010). These mussels dominate the biomass of hydrothermal communities at several vent sites, thus playing a major role in energy transfer in these ecosystems (Van Dover, 2000). Diffuse vent environments display a complex combination of abiotic constraints with respect to the physiological requirements of these mussels (e.g. temperature limits, oxygen depletion and low pH limitation for carbonate mineralization) and the energy requirements of their symbionts (e.g. sulfide and oxygen availability, and alternative electron donors like methane or hydrogen in dual or mono-symbioses) (Johnson et al., 1994; Le Bris et al., 2006; Nees et al., 2009). A better understanding of the growth dynamics of these foundation species is thus needed if we want to appreciate their role in ecosystem functions. Furthermore, we need to elucidate the links between growth dynamics and habitat conditions. The capacity of recruits, not only to settle and survive but also to grow, ultimately governs the ability of this species to recolonize after vent habitat disturbances caused by volcanic eruptions or by anthropogenic impacts.

Bathymodiolus brevior and *Bathymodiolus thermophilus*, two species from Pacific hydrothermal vents, have been shown to grow according to a von Bertalanffy model (Schöne and Giere, 2005; Nedoncelle et al., 2013). With a shell growth rate up to 4 cm per year in the juvenile stage, these species form large mature beds on the seafloor within a few years, reaching an asymptotic size at about 18 years. These studies also revealed spring-neap periodicities in the daily shell growth rate of the two species (i.e. 14–28 days) and proposed periodic changes in the mussel habitat conditions as the probable cause of this variability. As temperature records near diffuse venting sources commonly show, the fluid-seawater mixing conditions in diffuse vent habitats exhibit periodic variations, with spring-neap tidal cyclicity or modulation over longer periods (Chevaldonné et al., 1991; Johnson et al., 1994). No detailed mechanism was however established to support the relationship between growth cyclicity and habitat temperature fluctuations and explain the inferred tidal effects on growth rates. More generally, very little is known on the abiotic factors influencing growth in vent habitats.

Bathymodiolus thermophilus is an endemic species of the East Pacific Rise (EPR), an area that undergoes frequent volcanic eruptions, with massive lava flows leading to the local extinction of invertebrate populations established around vents (Shank et al., 1998; Mullineaux et al., 2012). The 9°50'N vent field was disturbed by massive eruptions in 1991 and in January 2006 (Soule et al., 2007). In early 2006, the massive volcanic eruption eradicated *B. thermophilus* from an area measuring several square kilometers, while dense mussel beds persisted at the periphery of the lava flow (Fornari et al., 2012). After a delay in larval recruitment (Mullineaux et al., 2012), mussel populations reestablished on new habitats. This recolonization sequence, similar to that observed 15 years earlier (Shank et al., 1998), provided an opportunity to better understand how growth dynamics are influenced by environmental conditions at different time scales.

In this paper, we examine the temporal characteristics of the mussel habitat along with shell growth variations on specimens collected from two large populations from the 9°50'N area; a new population at the Bio-9 site that was covered by lava during the last eruption and a second population at the V-vent site, 5.8 km south of Bio-9, that was not reached by the lava flow. The size distribution of a large sample from the new Bio-9 population was examined in the context of the von Bertallanfy shell growth model. Based on a sclerochronology method calibrated with *in situ* fluorescent marking (Nedoncelle et al., 2013), the daily growth rate was assessed for individuals from the two sites over periods of several days, and compared to short-term fluctuations of environmental variables (temperature, sulfide, oxygen and pH). The comparison between oceanographic data and temperature recorded during the post-eruption monitoring program (NSF Ridge 2000) and shell growth records of V-vent samples was used to examine how growth can be modulated over the long-term by hydrodynamic forcing at regional and ridge scales. A first analysis of the potential links between physico-chemical constraints in the mussel habitat and growth patterns is proposed on this basis, paving the way for future experimental investigation of abiotic influences on growth and, therefore, on the reestablishement of high-biomass populations of these foundation species in disturbed hydrothermal environments.

2. Materials and methods

2.1. Mussel collections

Individuals of *Bathymodiolus thermophilus* used for size-distribution and sclerochronological analyses were collected during three cruises using the deep-sea manned submersibles Nautile (R/V Atalante cruises MESCAL1 in April–May 2010 and MESCAL2 in March 2012) and Alvin (R/V Atlantis cruise AT2610 in January 2014). Biological sampling was conducted on two vent sites of the EPR: V-vent (09°47.3'N, 104°17.0'W, 2513 m depth) located at the southern exterior edge of the lava flow that covered the area in early 2006 and Bio-9 (9°50.3'N, 104°17.5'W, 2508 m depth) located within the area impacted by the eruption (Soule et al., 2007) (Suppl. Fig. 1a).

In 2010, 35 mussels were collected at V-vent from a single large mussel bed covering about 50 m^2 of a diffuse vent area on the basaltic seafloor. The area had been previously visited in 2007 by Mullineaux et al. (2012), who reported large mature mussel beds representing pre-eruption populations (Suppl. Fig. 2a). This same bed was sampled in 2010 as described in Nedoncelle et al. (2013) (Suppl. Fig. 2b).

In 2012, individuals were collected from a large mussel bed surrounding a *Riftia pachyptila* bush at Bio-9 (Suppl. Fig. 1b), within a few tens of meters from a black smoker complex. Four collections composed of 43, 67, 84 and 28 individuals were collected in bioboxes from three different locations in this area (Suppl. Table 1). The mussels used for sclerochronological analyses belong to the first and third mussel collections.

A size-distribution analysis was performed on the 222 individuals of *B. thermophilus* collected at Bio9. Each shell was measured along its maximum growth axis, from the ventral margin to the hinge. The age of the most abundant class was estimated from the growth model previously established using in situ calcein marking of shells at V-vent (Nedoncelle et al., 2013). We similarly

Table 1
Collection and labeling of the ten V-vent samples and six Bio-9 samples used for sclerochronology analysis. For each shell, the number and position of the measured shell growth increments are precised.

Collection site	Shell number	Date of cage deployment	Date of recovery	Marking date	Measured growth increments
V-vent: Center	Vvent-1	–	05/13/10		10 increments from v. margin
	Vvent-2	–	05/13/10		10 increments from v. margin
	Vvent-3	–	05/13/10		10 increments from v. margin
	Vvent-4[a]	–	05/13/10		10 increments from v. margin
	Vvent-5[a]	–	05/13/10		10 increments from v. margin
	Vvent-6[a]	–	05/13/10	05/03/10 *in situ*	whole shell length & 10 increments from v. margin (after mark)
	Vvent-7[a]	–	05/13/10	05/03/10 *in situ*	whole shell length & 10 increments from v. margin (after mark)
	Vvent-8	–	05/13/10		10 increments from v. margin
	Vvent-9[a]	–	05/13/10		whole shell length & 10 increments from v. margin
V-vent: Periphery	Vpheriph[a]		05/13/10		whole shell length
Bio-9	Bio9-1	03/22/12	01/15/14	on board	5 increments before mark
	Bio9-2	03/22/12	01/15/14	on board	5 increments before mark
	Bio9-3	03/22/12	01/15/14	on board	5 increments before mark
	Bio9-4	03/17/12	03/22/12	on board	5 last increments after mark
	Bio9-5	03/17/12	03/22/12	on board	5 last increments after mark
	Bio9-6	03/17/12	03/22/12	on board	5 last increments after mark

[a] Individuals used in Nedoncelle et al. (2013) to establish the von Bertallanfy model.

estimated the age of smaller individual classes, assuming that the model applies for all collected individuals.

2.2. Sclerochronological analyses

Circalunar growth rates (later referred as 'daily growth rate') were quantified as described in Nedoncelle et al. (2013). This value is defined by the increment width between two successive shell growth striae. Table 1 summarizes the sclerochronological analyses performed on ten individuals from V-vent and six from Bio-9.

For V-vent, the analysis was done on ten shells over the ten days preceeding their collection. Nine shells were collected in the center of the mussel bed, the last one from the periphery. On the first day, autonomous sensors were deployed on the mussel bed to monitor environmental conditions and a patch of individuals was marked *in situ* with calcein. Two of the collected shells displayed a well-defined fluorescent line, confirming the formation of one increment per day (Nedoncelle et al., 2013). For these shells, daily growth rates were quantified from the ten increments between the marking line and the ventral margin. For unmarked shells, the ten increments preceding the ventral margin were measured. This sclerochronology data set encompass the six shells used by Nedoncelle et al. (2013) for the growth model definition and four additional shells.

A similar short-term analysis was done for six individuals from Bio-9, but in this case all individuals were marked on board and redeployed in cages. Two cages were successively deployed in 2010 on the Bio9 mussel bed (Table 1). The first cage was positionned close to the *in situ* sensors deployed on the mussel bed and recovered five days later (see Section 2.3). Three shells of mussels recovered alive from this cage were analyzed (Table 1). The second cage was deployed on the same location, immediately after recovery of the first cage and recovered during the R/V Atlantis AT2610 cruise in January 2014 (Suppl. Figure 1c). Three live mussels recovered from this cage were included in the analysis.

The daily shell growth was quantified, in both cases, over the five-day deployment period of in situ sensors. Accordingly, the width of the five growth increments formed between deployment (03/17/2012) and recovery (03/22/2012) was measured for the three marked individuals recovered in 2012 (Table 1). We assumed that (1) depressurization and marking did not affect daily growth, and (2) no growth occurred out of *in situ* conditions. For the second set of individuals, marked at the end of the environmental monitoring period (03/21/2012), we measured the width of the five increments preceeding the well-defined fluorescent mark. A significant growth after marking made the quantification easier than on individuals recovered after only a few days. This method also circumvents the effet of depressurization and marking on the measured daily growth rates.

Finally, we used the long-term sclerochronological data series obtained by Nedoncelle et al. (2013) for four V-vent individuals to analyze the correlations between growth rate and environmental variables monitored under the LADDER project (Section 2.5). These three to four-year long series were obtained over the whole length of the shell, from the outer rim toward the umbo, for four V-vent mussels, three from the center of the patch (C-shells) and one from the periphery (P-shells).

2.3. Sulfide, pH and temperature measurements

In situ sulfide and pH measurements were acquired continuously at discrete locations in the V-vent and Bio-9 mussel beds using autonomous electrochemical sensors specially designed for vent habitat studies (Le Bris et al., 2001, 2012; Contreira-Pereira et al., 2013). The devices were deployed in the centers of the mussel beds and recovered at the time of mussel sampling (Suppl. Fig. 2b, c). The potentiometric (SPHT, NKE SA) and voltammetric (SPOT, NKE SA) data loggers were run autonomously using the Winmemo software at rates ranging from 2 to 4 measurements per hour, to avoid memory saturation of the voltammetric sensor. Temperature records were obtained simulateously using autonomous probes (S2T6000, NKE SA), which 1.5 mm-diameter tip was tightly linked with the electrodes.

In 2010 at V-vent, combined potentiometric sensors were used to monitor both pH and free sulfide concentration (H_2S+HS^-) as described in Le Bris et al. (2012). Temperature, pH and sulfide were monitored with a frequency of 2 meas. per hour over 10 days, with the sensors deployed from 05/03/2010 at 20:30 to 05/14/2010 at 23:00 in the mussel bed. In 2012, a voltametric sensor equipped with a silver electrode was substituted for the potentiometric sulfide sensor to improve measurement accuracy and allow quantitative comparison with a conservative mixing model (Contreira-Pereira et al., 2013). Simultaneous records of temperature and sulfide were acquired during five days at Bio-9 from 03/17/2012 to 03/21/2012 every 5 and 15 min respectively. No pH data

are available from 2012 due to electrode failure.

2.4. Estimates of sulfide consumption and maximum oxygen concentration

The measured concentrations of sulfide in mussel beds were compared to the predictions of a conservative model, using temperature as a proxy for the vent fluid-seawater mixing ratio as done in Le Bris et al. (2006). In the conservative mixing assumption, the sulfide concentration is defined by:

$$[H_2S]_{model} = (T - T_{sw})*R \quad (1)$$

where T is the temperature in °C and T_{sw} the temperature of background seawater (2.0 °C), R is the ratio between the sulfide concentration and temperature anomaly characterizing the vent fluid fuelling the assemblage. We assumed an R value of 13.2 μM °C^{-1}, as done by Contreira-Pereira et al. (2013). This value is derived from the maximum sulfide-to-temperature anomaly ratio achieved over the monitoring period in the studied area in 2012.

As done previously from discrete measurement data sets (Johnson et al., 1994; Le Bris et al., 2006; Le Bris et al., 2003), deviations from this linear model are considered to reflect sulfide depletion in the mixing gradient and are attributed to biological consumption by free-living microbes or symbiotic bacteria. In the absence of metals, abiotic oxidation of sulfide by oxygen is comparatively considered sluggish, though traces of iron can significantly increase this rate (Zhang and Millero, 1994). Temporal changes in the consumed sulfide concentration can be determined on this basis, according to Eq. (2):

$$[H_2S]_{consumed} = [H_2S]_{model} - [H_2S]_{measured} \quad (2)$$

Since no in situ sensor was available for oxygen, estimates were obtained assuming that the oxygen concentration follows a linear trend with temperature, as shown by Moore et al. (2009) data for EPR 9°50'N habitats. We use the slope and intercept of the linear regression defined from data acquired at different locations of the Bio-9 site in 2012, within the mussel bed and in the transition zone occupied by mussels and tubeworms (Suppl. Fig. 3). Measurements were obtained using the cyclic voltammetry method described in Luther et al. (1999), with a gold-amalgam electrode connected to a miniaturized potentiometer (SPOT-L, NKE SA) and attached to the tip of a temperature sensor (S2T6000 DH, NKE).

Accordingly, oxygen concentration was estimated from temperature (T) using the linear relationship:

$$[O_2]\,(\mu M) = 148.0–11.4\,T\,(°C) \quad (3)$$

In this model oxygen equals zero at 13 °C, which is similar to the 12 °C limit for oxygen in the vent fluid-seawater mixing zone defined by Moore et al. (2009) for the 9°50'N Marker7 site in 2007. The linear model assumes conservative mixing for oxygen above this threshold. These estimates therefore reflect the maximum concentration of oxygen for a given temperature, without accounting for eventual local consumption.

2.5. Frequency analyses and correlation of growth patterns with physical tracers

Selected temperature records (Mullineaux et al., 2012) and other physical oceanography data (Liang and Thurnherr, 2012) recorded during the NSF LADDER project (http://www.whoi.edu/projects/LADDER/) were used to examine correlations between sclerochronological records and environmental cyclicities. The long-term data sets are available from the Marine Geoscience Data System (http://www.marine-geo.org/). For our purpose, we selected a 325-day temperature series acquired at a rate of 1 measurement per 15 min on the bottom, within a large mussel bed at V-vent from 12/31/2006 to 11/21/2007 (Suppl. Fig. 2a). In addition, we used a long-term time series of near-bottom current velocities recorded at 9°50'N every 20 min from 04/11/2006 to 11/27/2007, i.e. the 388.5-day record of the NA2 instrument deployed ~20 m above the EPR crest topography (24 m above the floor of the shallow graben; Thurnherr et al., 2011).

A pressure record obtained under the Ridge 2000 program at 9°51'N–104°17'W was also used for investigating the diurnal and semidiurnal tidal influence. Pressure measurements included in the analysis are from to a 471-day period from 02/27/2007 to 06/12/2008 sampled at a rate of 1 measurement per minute at 9 °51'N–104°17'W.

The segment-scale oceanographic measurements obtained during LADDER are detailed in Jackson et al. (2010) and Thurnherr et al. (2011). We selected the records (temperature, current and pressure) acquired closest to our study site and analyzed the data to compare their periodicities with growth periodicities. Spectral analysis using Fast Fourier Transforms was performed using the multi-taper method (Thomson, 1982) and robust red noise modeling, as implemented in the singular spectrum analysis multi-taper method (SSA-MTM) toolkit (Ghil et al., 2002). We applied the MTM to the raw time series over the entire period of recording for temperature, pressure and current velocity. The FFT analysis of pressure records (1 meas./min) was performed on 1 h-averaged values, in order to limit the data set size.

From the long-term time series, the correlations of shell growth with temperature and current-velocity components were examined for each individual shell using the Spearman test (ST). To limit the influence of high-rate fluctuations, daily shell growth series were smoothed applying a moving median with a period of 14 days (i.e. a whole fortnightly cycle, Suppl. Fig. 4). The correlations between pressure and shell growth rate variability were also investigated applying the Spearman test to variations in the maximum daily pressure. Compared to mean daily pressure, variations in the maximum daily pressure are more representative of the dominant periodicities of the tidal forcing.

3. Results

3.1. Size and age structure of the new population at Bio-9

In April–May 2010, 4.3 years after the eruption event, dispersed small mussels were distinguishable on video at Bio-9 and large aggregations of *R. pachyptila* were already present (Suppl. Figure 1a). In March 2012, 6.1 years after the eruption, large aggregations of adult-size mussels covered the basaltic seafloor in diffuse flow areas (Suppl. Fig. 1b). The histogram of shell length for the population sampled in 2012 revealed one dominant class size (54–96 mm) together with smaller individuals (Fig. 1). Applying the von Bertalanffy model established previously (Nedoncelle et al., 2013), the most abundant shell size class ($E_{t+\Delta t}$=72 mm) sampled in March 2012 is estimated to be 1.3 ± 0.1 years old (16 months).

The smaller individuals were present in two main groups: 30–51 mm and 9–15 mm, of decreasing abundance with size. The smallest class was only represented in one collection, while the intermediate class was found in 3 of the 4 samples (Suppl. Table 1). For the two groups, the von Bertalanffy model estimates are, respectively, 0.2 years ± 0.1 (2.1 months) and 0.7 years ± 0.1 (8.3 months).

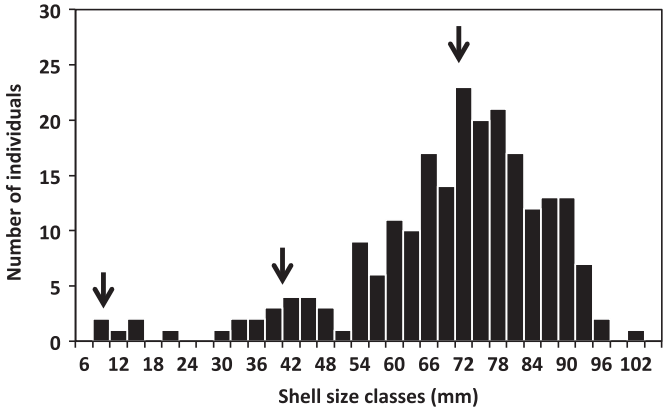

Fig. 1. Shell length histogram of the population sampled in 2012 at Bio-9 (222 individuals). Black arrows indicate the three main classes considered for age estimates.

Table 2
Daily increment width for individual shells analyzed from V-vent in 2010, over the 10 days of environmental parameter recording. Shell size (measured at the beginning of the experiment), daily mean ± SD, min and max increment width are mentioned.

Individual	**V-1**	**V-2**	**V-3**	**V-4**	**V-5**	**V-6**	**V-7**	**V-8**	**V-9**
Shell length (cm)	20.2	17.0	14.2	16.1	14.8	16.3	16.5	17.5	16.4
Date	**Daily increment width (μm)**								
05/04/10	26	41	43	26	46	24	35	21	36
05/05/10	18	48	28	13	74	13	35	25	30
05/06/10	15	87	29	15	26	17	13	10	96
05/07/10	13	43	24	20	60	11	19	15	55
05/08/10	18	24	37	24	47	11	23	23	22
05/09/10	32	27	23	24	16	12	29	13	18
05/10/10	42	48	42	22	45	5	19	35	22
05/11/10	24	37	23	27	31	9	17	23	16
05/12/10	17	36	39	20	30	10	43	11	12
05/13/10	47	55	50	50	77	42	81	57	39
Mean	*32*	*41*	*35*	*29*	*40*	*16*	*38*	*28*	*21*
Min	*17*	*27*	*23*	*20*	*16*	*5*	*17*	*11*	*12*
Max	*47*	*55*	*50*	*50*	*77*	*42*	*81*	*57*	*39*

Table 3
Daily increment width for individual shells analyzed from Bio-9 in 2012, over the five days of environmental parameter recording. Shell size, daily mean ± SD, min and max increment width variability are also mentioned. Shell size (measured at the beginning of the experiment), daily mean ± SD, minimum and maximent increment width are mentioned.

Shell reference	**Bio9–1**	**Bio9–2**	**Bio9–3**	**Bio9–4**	**Bio9–5**	**Bio9–6**
Shell length (cm)	9.2	7.5	7.2	10	5.3	4.1
Date	**Daily increment width (μm)**					
03/18/12	39	73	21	23	36	23
03/19/12	63	125	27	36	68	25
03/20/12	36	61	41	28	16	20
03/21/12	22	46	46	18	44	17
03/22/12	24	41	58	16	14	16
Mean	*37*	*69*	*39*	*24*	*36*	*20*
Min	*22*	*41*	*21*	*16*	*14*	*16*
Max	*63*	*125*	*58*	*36*	*68*	*25*

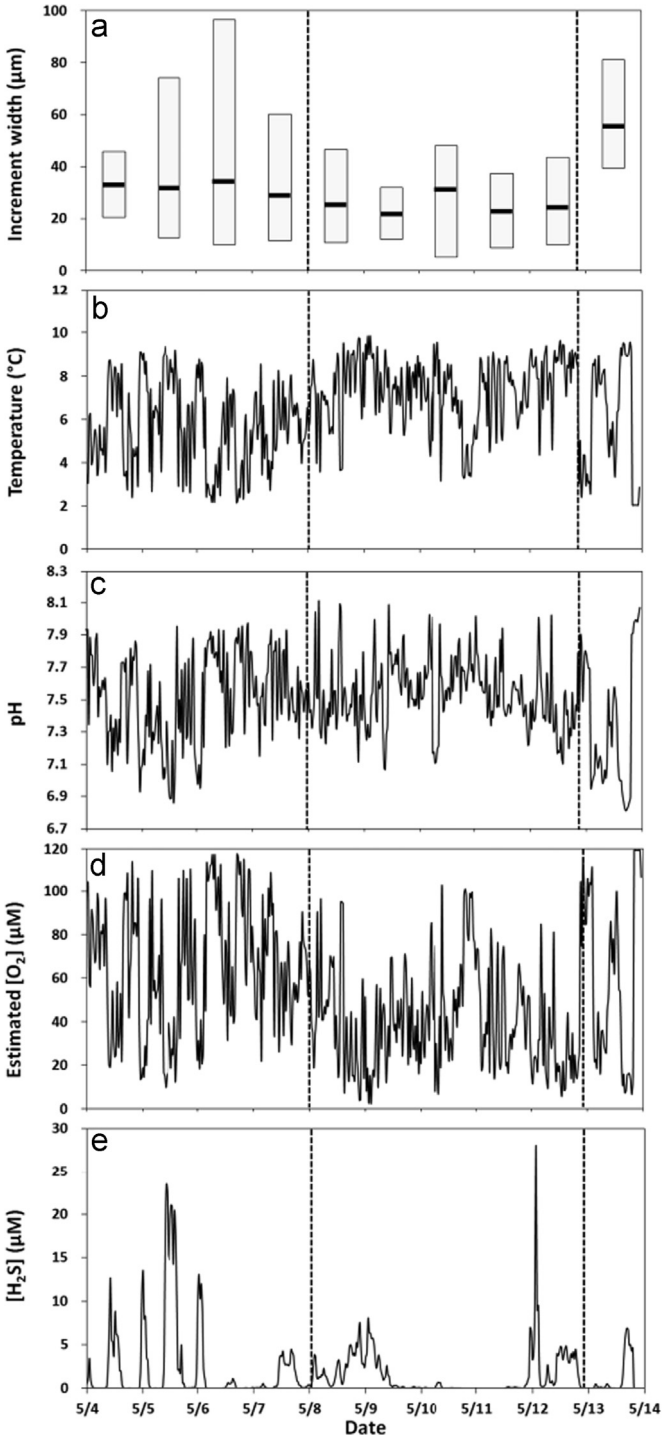

Fig. 2. Shell growth rate variations over ten days (mean, minimum and maximun daily increment width) for a pool of nine individuals from V-vent in 2010 (a). Corresponding fluctuations of habitat conditions monitored in the mussel bed: temperature (b), pH (c), estimated O_2 concentration (d) and measured sulfide concentration (e). The dashed lines delimitate the distinct fluctuation regimes discussed in the text.

3.2. Short-term variability in daily shell growth

Individual growth rates over the duration of short-term studies are presented in Table 2 (V-vent) and Table 3 (Bio-9). Significant differences were observed among individuals from the same patch, but consistent patterns were still observed between the two populations, with mean daily rates ranging from 16 to 41 μm d^{-1} at V-vent and 20–69 μm d^{-1} at Bio-9. Differences between individuals were reflected mainly in maximum rates (39–81 μm d^{-1} at V-vent and 25 to 125 μm d^{-1} at Bio-9), whereas variations in minimum rates were more limited.

Fig. 2a displays the mean daily growth variability over ten days (from 5/04 to 5/13/2010) for all V-vent individuals. Three time-intervals could be defined from this record. The first four days corresponded to higher growth rates with a median daily value

Table 4
Daily growth mean, median, first and third quartiles for the nine V-vent shells and the six Bio-9 shells, over respective habitat monitoring periods.

Site	Date	Mean ± SD	Med	Q1	Q3	*n*
V-vent	05/04/10	33 ± 9	35	26	41	9
V-vent	05/05/10	32 ± 19	28	18	35	9
V-vent	05/06/10	34 ± 33	17	15	29	9
V-vent	05/07/10	29 ± 19	20	15	43	9
V-vent	05/08/10	25 ± 10	23	22	24	9
V-vent	05/09/10	22 ± 7	23	16	27	9
V-vent	05/10/10	31 ± 15	35	22	42	9
V-vent	05/11/10	23 ± 9	23	17	27	9
V-vent	05/12/10	24 ± 13	20	12	36	9
V-vent	05/13/10	55 ± 15	50	47	57	9
Bio-9	03/18/12	36 ± 20	30	23	38	6
Bio-9	03/19/12	57 ± 38	50	29	67	6
Bio-9	03/20/12	33 ± 17	32	22	40	6
Bio-9	03/21/12	32 ± 14	33	19	45	6
Bio-9	03/22/12	28 ± 18	20	16	37	6

ranging between 29 μm and 34 μm d^{-1} for the nine analyzed shells, and large increments for three individuals (from 74 μm to 96 μm d^{-1}) (Table 2). The five following days were characterized by a lower shell growth rate for all nine individuals (< 48 μm d^{-1}), and a mean daily growth rate ranging between 22 and 31 μm d^{-1} (Table 4). A high daily growth rate was observed again on the last day for all studied shells with a mean increment width of 55 μm d^{-1}.

The growth rates of the six Bio-9 mussels reflected a similar variation range over the corresponding 5-day record in 2012 (3/18-3/22/2012), with a maximum value of 73 μm d^{-1}, a minimum of 14 μm d^{-1} and a mean daily growth rate ranging from 28 to 44 μm d^{-1} (Fig. 3a and Table 3).

3.3. *Short-term habitat physico-chemical variability and sulfide consumption*

Temperatures recorded over ten days in 2010 in the sampled mussel assemblage at V-vent ranged from ambient seawater (2.0 °C) to a maximum of 9.9 °C with a median value of 6.8 °C over the ten-day period (Fig. 2b). The FFT-analysis performed on this data set shows a marked semi-diurnal cyclicity (Suppl. Fig. 4). During the first four days of the shell growth record (from 05/04 to 05/07/2010), temperature substantially fluctuated (with first and third quartiles respectively of 4.1 °C and 7.3 °C) but the median temperature remained relatively low with a value of 5.6 °C. Conversely, during the five subsequent days (from 05/08 to 05/12/2010), conditions were warmer with a median value of 7.5 °C and a reduced amplitude of the fluctuation (first and third quartiles of 6.4 °C and 8.5 °C, respectively). During the last day of the monitoring period (05/13/2010), the median temperature decreased to 6.9 °C and temperature again displayed larger fluctuations (first and third quartiles of 3.4 °C and 8.7 °C, respectively).

The 10-day pH record in the V-vent mussel bed had a median value of 7.5, as well as minimum and maximum values of 6.9 and 8.0, respectively (Fig. 2c). Like temperature, pH also exhibits strong semi-diurnal variability (FFT analysis, suppl. Fig. 4b). While the largest temperature fluctuations were observed in the first period, the corresponding pH undergoes only moderate variation with first and third quartiles of 7.3 and 7.7, respectively. In the second period, the pH ranged between 7.4 and 7.7 along with more stable thermal conditions, while more substantial pH fluctuations were

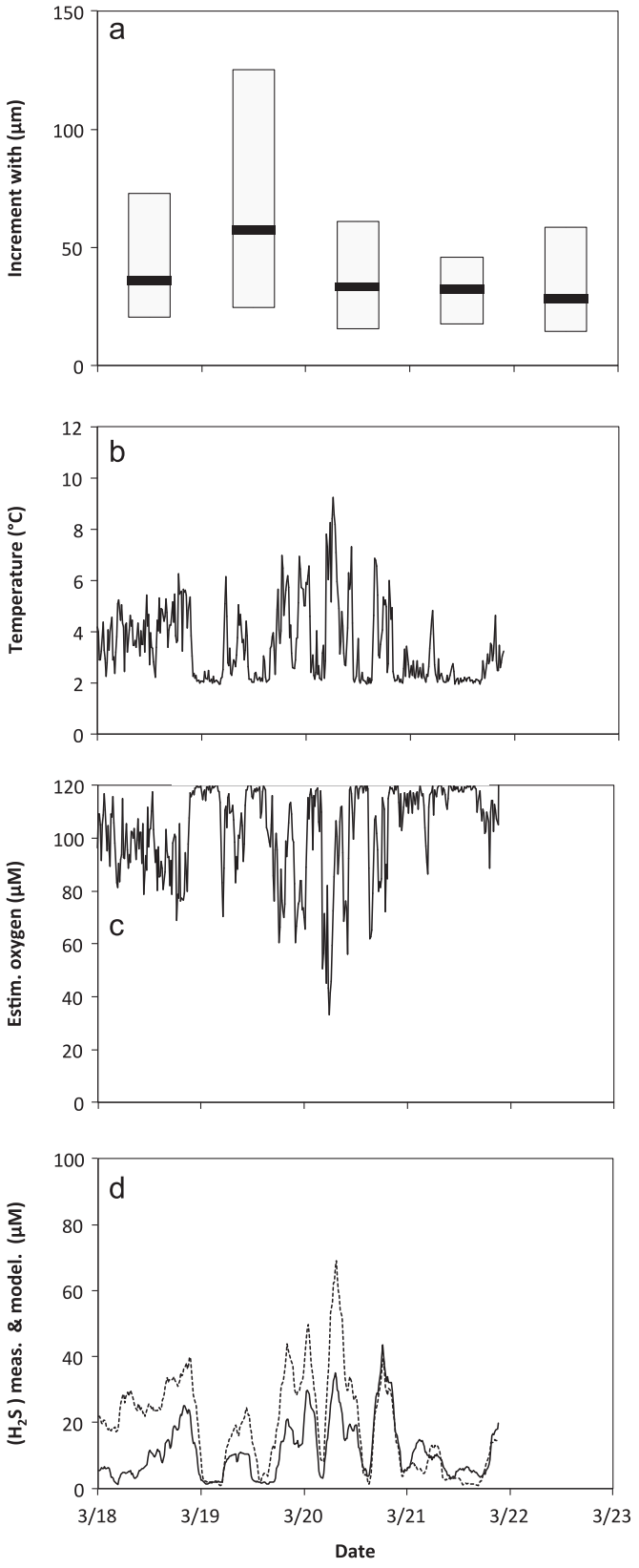

Fig. 3. Shell growth rate variations over five days (mean, minimum and maximun daily increment width) for a pool of six individuals from Bio-9 in 2012 (a). Corresponding fluctuations of habitat conditions monitored in the mussel bed: temperature (b), estimated O_2 concentration (c) and measured and modeled (dotted line) sulfide concentrations (d). Sensors were recovered one day before mussel sampling.

observed in the third period (first and third quartiles of 7.0 and 7.6, respectively). While the amplitudes of the pH fluctuations were similar in the first and second periods, pH more frequently lied in the higher and lower end of the range (i.e. below Q1 and above Q3) in the first period than in the second period (Fig. 2c).

According to the imposed inverse linear relationship with temperature, O_2 estimates also displayed semi-diurnal fluctuations (Suppl. Fig. 4c). The highest oxygen concentration occurred in the first 4 days with a mean of 65 μM and maxima approaching the background deep-sea water concentration (Fig. 2d). The same time period was also characterized by large fluctuations with first and third quartiles of 41 μM and 88 μM, respectively. During the five following days, the estimated median oxygen concentration dropped to 38 μM, and the variability was reduced as well, with first and third quartiles ranging between 22 μM and 54 μM. On the final day, the median value increased again to 46 μM, and the fluctuation amplitudes also increased (Fig. 2d).

Measured sulfide concentrations were also highly variable with marked semi-diurnal fluctuations (FFT analysis; Suppl. Fig. 4d). Sulfide concentration during the first 4 days varied from below the detection limit (1 μM) to a maximum of 24 μM (Fig. 2e), with sulfide pulses alternating with non-sulfidic periods. During the next 6 days, sulfidic conditions still occured intermittently, although less frequently (Fig. 2e). In this second period, the concentration of sulfide spiked up to 28 μM, but most of the time remains below the quantification threshold of the potentiometric sensor (c.a. 20 μM). Similar low sulfidic conditions are observed during the last day.

At Bio-9 in 2012, both temperature and sulfide concentration exhibited fluctuations with a period of 12 h (Fig. 3b,d). The measured sulfide concentrations ranged between <1 μM and 63 μM. Comparison with the model estimates, based on conservative mixing, indicated that consumption of sulfide in the vicinity of mussels also displayed strong fluctuations, ranging from 0 to 100% of the expected sulfide concentration (Fig. 3d). The absolute decrease in concentration ranged from 0 to 53 μM. The estimated oxygen concentration was also highly variable but lied near the high end of observed concentrations at 9°50'N vents in the background seawater (e.g. without temperature anomaly), with a mean of 108 ± 17 μM, and minimum and maximum values of 43 μM and 126 μM, respectively (Fig. 3c).

3.4. Growth cyclicity and long-term variability of physical factors

The 486-day daily growth rate record exhibited a significant period of 14 ± 2 days on average for the nine V-vent shells, and a less significant period around 26 days (Fig. 4). The FFT analysis also revealed significant period near 60 days and at lower frequencies.

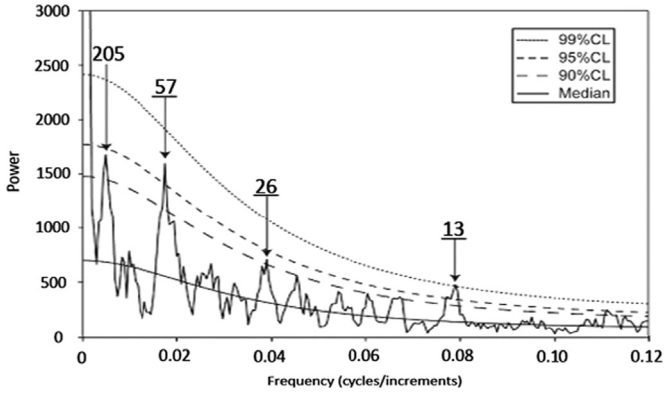

Fig. 4. 2π-MTM power spectrum of the daily growth series acquired over the whole shell length for one *B. thermophilus* shell collected at V-vent in 2010.

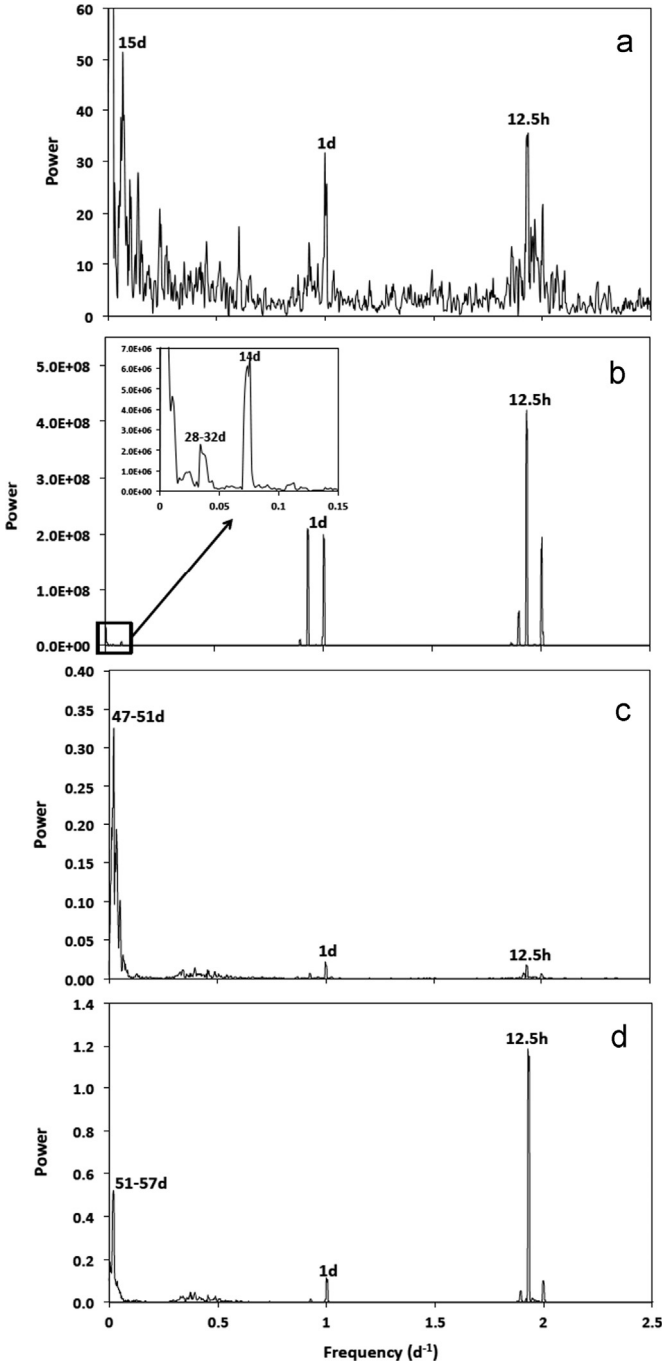

Fig. 5. 2π-MTM power spectra of long-term environmental data series acquired at V-vent during the Ridge 2000 program: temperature in a mussel bed (a); pressure (b) and N–S (c) and E–W (d) current velocities monitored 20 m above the ridge crest.

The FFT analysis of the long-term temperature time-series at V-vent indicated a significant period at 15d, in addition to dominant diurnal and semidiurnal periods (Fig. 5a). Two of the four *B. thermophilus* shells display a significantly positive correlation between growth rate and temperature fluctuations over the period matching the temperature time-series (i.e. from Dec. 2006 to Nov. 2007) (Table 5). Both were located in the center of the clump. The two other shells (one from the center and one from the periphery) do not display any significant relationship between growth rate and temperature.

Spectral analysis of the pressure time series revealed common periodicities with shell growth and temperature fluctuations

Table 5
Spearman correlation tests between daily shell growth rates for V-vent mussels and E–W current velocity, N–S current speed, temperature and maximum pressure.

Reference	Shell length (cm)	E–W current velocity	N–S current velocity	Temperature	Maximum pressure
V-6	16.3	0.00	0.01	0.00	−0.11
V-7	16.5	−0.13*	0.26*	0.17*	0.21*
V-9	16.4	−0.24*	−0.23*	0.34*	0.31*
V-periph	15.4	0.14	0.03	0.02	−0.19*

* Indicate significant correlations (p-values < 0.05). V-6, V-7 and V-9 shells were collected in the center of the mussel bed and V-periph at the periphery (Table 1).

(Fig. 5b). The most prominent frequencies were 12.5 h and 1d, but a peak at 14-day frequency and a less pronounced one at 28–32-day frequency were also displayed. Two of four *B. thermophilus* shells displayed a significantly positive correlation between growth rate and daily pressure maxima in the time-interval of pressure measurements (Table 5). One of two remaining shells from the center of the bed did not exhibit a significant relationship, whereas the shell from the periphery displayed a negative correlation with pressure variations.

FFT analyses on selected current-velocity time-series revealed currents with major periodicities of 47–51 and 51–57 days, for the N–S (Fig. 5c) and E–W (Fig. 5d) velocity components, respectively. These fluctuations again combined with semi-diurnal cyclicity, which largely dominated the variation of current velocity in the E–W direction, while along the N–S direction the low frequencies were more pronounced. No peak near the 15-day period was observed in the velocity spectra. Two shells from the center of the mussel patch displayed a negative relationship between growth rate and current velocity along the E–W axis. The growth of a third shell located in the center of the patch did not correlate significantly with current velocity along the E–W axis (Spearman test, p-value > 0.05), and this was also the case for the shell collected at the periphery. The two shells from the center of the mussel bed also displayed significant correlations with the N–S axis current velocity (Spearman test, p-value < 0.05) (Table 5). However, one of the two shells displayed a negative relationship ($r < 0$) while the second displayed a positive relationship ($r > 0$). Similar to the E–W axis velocities, the two remaining shells, one from the center and the other from the periphery, did not exhibit significant correlation between growth rate and current velocity along the N–S axis (Table 5).

4. Discussion

4.1. Rapid growth of first settlers and potential limitations to successive settlements

The post-eruption colonization dynamic observed between May 2010 and March 2012 at Bio-9 confirms *B. thermophilus* as a late colonizer in the species succession sequence, similar to reported after the 1991 eruption (Shank et al., 1998). In 2010, abundant *R. pachyptila* populations had already established, though mussels were still scarce in the area (Suppl. Fig. 1a). The size histogram of the population collected at Bio-9 depicts a mature colony, while the observation of sparse mussels at this site in 2010 was consistent with the delayed reestablishment of this species after the eruption (Suppl. Fig. 1a). These observations correspond with estimates of older individuals being 1.3 year-old in 2012, based on the von Bertalanffy model previously established for an undisturbed population at V-vent (Nedoncelle et al., 2013). The size structure of the sampled mussel bed at Bio-9 in 2012, furthermore, highlights a main size-class indicative of a major succesfull settlement event followed by rapid growth (56 mm yr^{-1} on average). This initial successful settlement would have occurred around 4.6 years after the eruption, similarly to previous post-disturbance observations at 9°50'N on the EPR (Shank et al., 1998).

The occurrence of smaller size classes are more subtle to interpret. One interpretation is that three successive distinct cohorts settled at time intervals of 6–8 months, following a first settlement at the end of 2010 (c.a. 4.8 years after the eruption). This scenario is consistent with the hypothesis of discontinuous pluriannual reproduction, as suggested by histological analysis of female oocytes revealing constant diameters not only in single individuals, but also between different mussels from the same site or from different sites (P. Tyler and F. de Busserolles pers. obs.).

This discontinuous, pluriannual reproductive strategy together with rapid initial growth could reflect adaptations to the instability of the environment characterizing opportunistic species (Eckelbarger, 1994), leading to fast increase in population and biomass after the initial settlement. However, the decrease in abundance of assumed younger cohorts raises the question of settlement limitation for new recruits after the establishment of the first adults. The predation influence exerted by mussels on their own larvae possibly affects the local establishement of new cohorts, as suggested by Lenihan et al. (2008), and could partly explain a low recruitment efficiency at Bio-9 after the initial colonization stage.

Furthermore, the existence of successive cohorts is not firmly established, since the smaller class is not found in all 4 samples, but only at one location where the size range was broad with few individuals from each class (Suppl. Table 1). Without a large sampling effort, involving different locations at Bio-9, it is thus not possible to demonstrate this periodic settlement hypothesis. The possibility that individuals settled at the fringe of the suitable habitat area would have experienced growth limitation cannot be dismissed. In any case, the low number of small individuals indicates that younger cohorts are limited within the resettled population. The situation at Bio-9 appears to differ from that described by Van Dover (2002) for active South-EPR sites where juveniles were more numerous than adults.

These results are consistent with the idea that the primary limiting factor to the reestablishment of large mussel populations is the capacity of *B. thermophilus* to recruit, as experimentally demonstrated using settlement surface deployed in the disturbed area in the first two years after the eruption (Mullineaux et al., 2012). Once initial settlement limitations are overcome, habitat adequacy for growth is the key to the rapid development of populations. Noticeably, the observation of juveniles on basalt blocks at 9°50'N on the EPR were made as early as January 2008. These early settlers did not form adult populations at the Tica site revisited 10 months later, suggesting that habitats could be or may have become unfavorable for growth in the following months (N. Le Bris pers. obs.).

4.2. Short-term growth variability and habitat fluctuation regimes

A better description of habitat conditions favorable to growth is thus needed if we are to understand how these foundation species reestablish their populations and drive chemosynthetic biomass production. Common features in daily growth variability are shared between the recent (disturbed site) and mature (undisturbed site) settlements. The difference in mean growth between the two sampled pools of mussels is consistent with the model establishing growth rate as function of size (Nedoncelle et al., 2013). However, individual shells from Bio-9 and V-vent

display similarly large fluctuations in daily growth rate over periods of a few days that can be used to examine the habitat factors potentially controlling shell growth.

Rapid semi-diurnal cycling between high and low temperatures, with marked transitions in physico-chemical parameters was prominent at both sites. Tidal cyclicity was first described in mussel beds on the Galápagos Ridge (Johnson et al., 1994). It was assumed to reflect short-term fluctuations in bottom current velocities and direction, influencing diffuse flow mixing plume (Scheirer et al., 2006). The idea is supported here by the diurnal and semi-diurnal periodicities occurring both in pressure and current velocities along the N–S and E–W axes that result in strong habitat physico-chemical fluctuations in the mussel beds.

What this study additionally shows is that the habitat of *B. thermophilus* undergoes significant modulations of the semi-diurnal tidal forcing on time scales of several days, resulting in modulations of the variability of temperature and several chemical parameters. In particular, periods of strong tidal fluctuations alternate with more stable conditions. Stable conditions can either reflect warm (e.g. high-hydrothermal contribution) or cool (low-hydrothermal contribution) periods. Several mussels of the V-vent pool grew faster during periods of strong fluctuations, while all of them had a low growth rate when warm and more stable conditions were established. At Bio-9, individuals displayed a high growth rate whenever they experienced stable cool conditions (low-hydrothermal conditions) or strongly fluctuating conditions, with maximum growth at the transition between the two regimes.

Despite the fact that the duration of measurements was too limited to allow a statistical treatment and for extrapolating the results over timescales representative of individual lifetimes, it is interesting to examine how the abiotic constraint regime's might influence energy allocation for shell growth. Childress and Fisher (1992) suggested that the tidal influence on mussel habitat would allow *B. thermophilus* to sustain significant uptake rates of sulfide for its symbionts, as this species is unable to concentrate sulfide as siboglinid worms do. In this study, measured sulfide levels within the Bio-9 mussel bed remained much lower than estimated from a conservative model using temperature as a proxy. Continuous measurements thus confirm that sulfide is effectively an energy limiting factor for mussel symbionts, as previously suggested from snapshot measurements (Johnson et al., 1994; Le Bris et al., 2006). While 100% of the sulfide flux was depleted in some periods at Bio-9, sulfide remained intermittently available. Conversely, in the stable warm regime at V-vent, H_2S remained low, suggesting substantial consumption, either by mussels or by other competing taxa including free-living bacteria. During this period at V-vent, the *B. thermophilus* environment was also poorly oxygenated with a mean estimate reaching only 41 μM. *B. thermophilus* symbionts might therefore also undergo oxygen limitations in this warm and stable regime, contrasting with fluctuating conditions where oxygen is available in alternance with sulfide. Limitation in energy supply for symbionts is thus expected to be more severe during warm regimes with low fluctuations than in colder but highly fluctuating regime.

Since mussels can digest symbionts or assimilate metabolic products independently of external conditions, host limitation should also be accounted. The permanently low oxygen conditions could also affect the host itself, though chemosynthetic mussels have capacities to survive hypoxia, with tolerance thresholds as low as 13 μM (Kochevar et al., 1992). In terms of oxygen, the conditions at Bio-9 appeared much more favorable, with permanently or intermittently high oxygen concentrations. Beyond oxygen, pH could also constrain the host metabolism. Even though mollusks are known to regulate the internal pH of their extrapallial fluid for shell mineralization (Crenshaw and Neff, 1969; Ip et al., 2006; McConnaughey and Gillikin, 2008), more energy has to be allocated to this process in low environmental pH conditions. Here, we show that high growth rates can be achieved in highly fluctuating regimes where pH variation as high as 1.5 units is experienced. In this case, repeated incursion near seawater pH may reduce the energy required for shell biomineralization, whereas more stable and warm conditions will be less favorable by maintaining pH in the lower range (Lutz et al., 1988; Tunnicliffe et al., 2009). The lowest growth rates in our study are associated with the later conditions.

This observation suggests that the continuous supply of sulfide is not the most relevant factor for the growth of *B. thermophilus*, as generally considered. Instead a sustained hydrothermal contribution, with low pH and low oxygen, may adversely affect the growth capacity of this species. Temporal variability rather appears to be a requirement for this species to establish high biomass assemblages, though this hypothesis would deserve further experimental demonstration.

4.3. Growth modulations driven by long-range hydrodynamic forcing

Previous studies have emphasized modulation in shell growth patterns of hydrothermal mussels over the lunar cycle (Schöne and Giere, 2005; Nedoncelle et al., 2013) and hypothesized an indirect influence of environmental conditions. This study confirmed that, at yearly scales, both habitat temperature and the daily growth of some individuals *B. thermophilus* indeed display similar 14-day spring-neap cyclicities, in addition to low-frequency variability around 60 days likely associated with the ridge-crest jets described by McGillicuddy et al. (2010), Thurnherr et al. (2011), and Lavelle et al. (2010) in this area. The significant correlation of growth patterns over more than a year with habitat temperature and current velocities for two individuals, and pressure for three of them, suggests a direct influence of environmental factors on growth. Despite the fact that this long-term analysis was limited to four individuals, these correlations provide additional clues to analyze the mechanisms lying behind this influence. Around diffuse flow vents where mussel thrive, temperature, oxygen and electron donor concentrations, as well as pH, correlate with the fluid-seawater mixing ratio (Johnson et al., 1994; Le Bris et al., 2006; Nees et al., 2009). Local variations of these parameters are therefore expected to be modulated by, both, the intensity of venting and the hydrodynamic forcing on local mixing gradients by bottom currents (e.g. as described in Scheirer et al., 2006).

For the individuals showing significant correlations with environmental factors, growth appears higher on average during warm periods (at the V-vent site) suggesting a favored growth in periods of high vent fluid flow. Since the 14-day frequency is not observed in the velocity time-series, current velocity modulations cannot explain this variability. Instead, a direct influence on mussel habitat conditions by the modulation of the local hydrothermal flow rate or its composition might be hypothesized (Pruis and Johnson, 2004) (Fig. 6a). 'Tidal pumping' driving the hydrothermal contribution to the local mixed layer was modeled by Crone and Wilcock (2005). The positive correlation of shell growth with temperature, also correlating positively with pressure, provides support for this hypothesis. Although no peak at 14-day was evidenced by Scheirer et al. (2006), temperature time-series from a mussel bed on the Mid-Atlantic Ridge also show evidence of spring-neap modulation (Sarrazin et al., 2014).

On the opposite side, strong current velocities with marked semi-diurnal tidal fluctuations (i.e. on the E–W axis) sometimes negatively correlate with growth at long-term scales. The highest tidal current velocities are thus not necessarily expected to represent the most favorable conditions for growth. This result emphasizes the complex downscaling of hydrodynamic influences

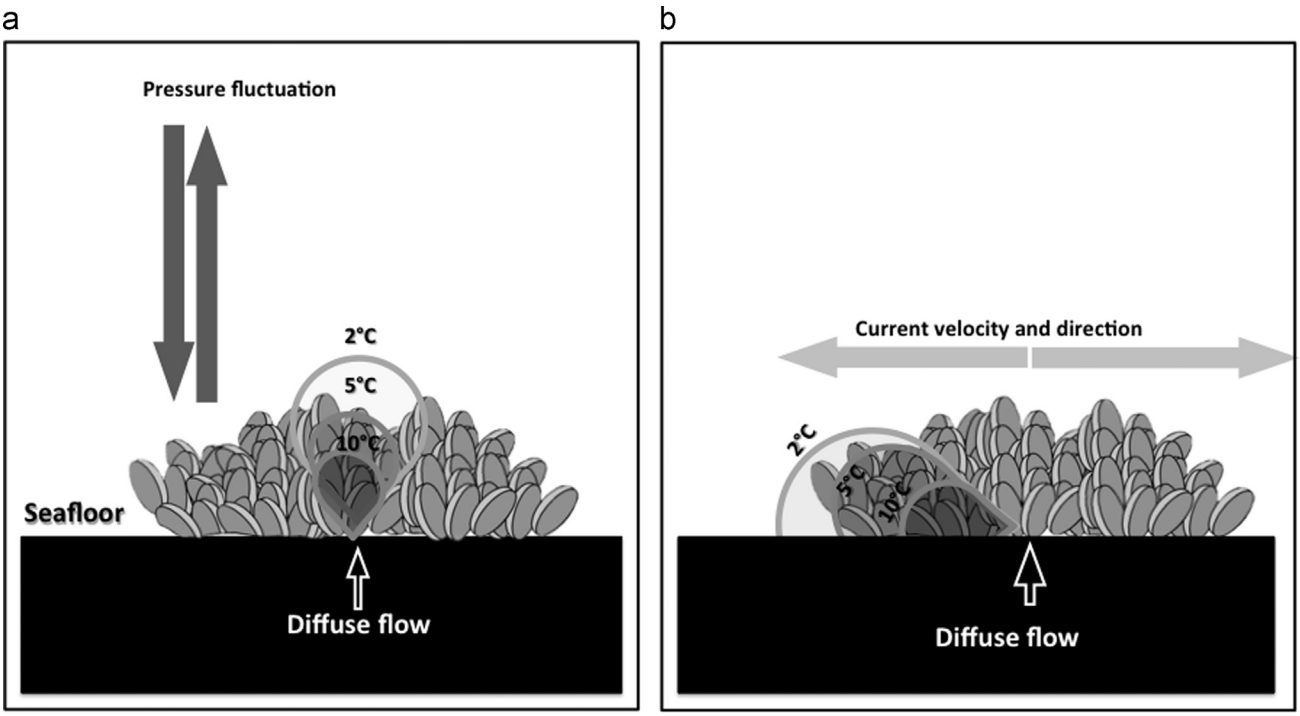

Fig. 6. Schematic representation of hydrodynamic forcings on the habitat of *Bathymodiolus thermophilus*. The fluctuations of abiotic factors in the mussel bed are governed by (a) the tidal pressure cycling modulating the fluid flow rate and (b) cyclic changes in current velocity and direction shaping the fluid mixing plume (b).

on mussel habitats due to the influence of mussel beds on shear stress, as shown in shallow water environments (Van Duren et al., 2006). In the case of *Bathymodiolus* mussel beds, it could indicate that stronger currents reduce seawater entrainment within the mussel bed, potentially leading to warmer and more stable conditions, less favorable for growth. Conversely, the low frequency cycles (periods around 60 days) recorded in shell-growth patterns have either positive, negative or no influence, which is qualitatively consistent with a distortion of the flow and asymmetric influence on growth within the mussel bed, though this result has to be statiscally strengthened from a larger number of indiduals.

It is thus suggested that shell growth dynamics integrate the signatures of (1) the lunar cycle influence on hydrothermal fluid flow intensity (Fig. 6a) and (2) the modulation of the semi-diurnal variability of bottom current velocities (Fig. 6b). Both types of hydrodynamic forcing are expected to govern the fluid mixing plume through the mussel bed, but will not imprint the individuals similarly in the bed. For mussels located at the periphery of the assemblage, their influence is likely to be less significant as sulfide is consumed along with the mixed fluid flowing through mussel aggregations, resulting in the absence of sulfide at the periphery and on top layers of the bed (Johnson et al., 1994; Fisher, 1990). Instead, mussels that are under direct influence of the fluid flow, with be strongly influence by the fluctuating regime induced by bottom currents.

5. Conclusions

Bathymodiolus thermophilus shells display marked periodicities in growth rates at circalunian (daily), fortnightly, monthly and longer cycles. The correlations between growth and environmental variability over different timescales supports the idea that daily growth rate variability reflects the combined effects of hydrothermal venting and oceanic current velocities, imposing different fluctuation regimes with regard to abiotic constraints. Several factors potentially limiting in situ growth are highlighted, the most important being sulfide limitation for symbionts and oxygen limitation for the host, while low pH conditions may also impact host energy allocation for shell mineralization.

The results draw attention to the fact that suitable habitat conditions for mussel growth should be examined on a temporal basis. These observations provide support for a direct hydrodynamic influence on mussel growth dynamics, on a monthly to yearly basis, even though combined effects of biological rhythms are not excluded. Furthermore, both local and regional drivers of habitat hydrodynamics are influencing mussel growth. Disturbance of these drivers is expected to have major consequences on the capacity of mussels to sustain growth in a given habitat.

Overall, the study emphasizes the need for integration of multiple observational scales in environmental studies. Dedicated in situ experiments are particularly needed to extrapolate these results over the lifetime of individuals and investigate habitat suitability for the reestablishment of mature mussel populations after habitat destruction by anthropogenic (e.g. mining) or natural (e.g. volcanic eruptions) disturbances.

Acknowledgments

We are grateful to the captains and crews of the R/V Atalante and R/V Atlantis, as well as the Nautile and Alvin operation groups. The chief scientists of the research expeditions MESCAL2010, MESCAL2012 (co-chief scientists N. Le Bris, F. Lallier, UPMC), and the scientific parties are gratefully acknowledged for their support and help during the cruises. We also acknowledge S. Sievert for the recovery of cages during the AT2610 cruise in January 2014. NSF Grants OCE-0424953 and OCE-0425361 (LADDER) and the Ridge2000 program are acknowledged for the availability of the data used in this study. The study benefited from the joint support of Fondation TOTAL and UPMC to the chair “Biodiversity, extreme marine environment and global change” and from the financial support of the CNRS and the Institute of Ecology and Environment (INEE) to the UMR8222 LECOB for participation to the cruises and

equipments, and from Ifremer for the vessel and submersible operations as part of the French Research fleet. K. Nedoncelle PhD grant has been supported by MESR and UPMC via the Doctoral School "Science de l'Environnement d'Ile de France" ED129 and L. Contreira-Pereira PhD grant was performed with the support of the EU Marie Curie ITN SENSENET contract n° 237868 (to NLB and LCP).

Appendix A. Supplementary material

Supplementary data associated with this article can be found in the online version at http://dx.doi.org/10.1016/j.dsr.2015.10.003.

References

Chevaldonné, P., Desbruyères, D., Le Haître, M., 1991. Time-series of temperature from three deep-sea hydrothermal vent sites. Deep-Sea Res. Part A Ocean. Res. Pap. 38, 1417–1430.

Chemosynthetic communities and biogeochemical energy pathways along the Mid-Atlantic Ridge: the case of Bathymodiolus azoricus. In: Le Bris, N., Duperron, S. (Eds.), Diversity of Hydrothermal Systems on Slow Spreading Ocean Ridges. Geophysical Monograph Series. Rona, P A, AGU, Washington, D C, pp. 409–429.

Childress, J.J., Fisher, C.R., 1992. The biology of hydrothermal vent animals: physiology, biochemistry, and autotrophic symbioses. Ocean. Mar. Biol. Annu. Rev. 30, 337–441.

Contreira-Pereira, L., Yücel, M., Omanovic, D., Brulport, J.-P., Le Bris, N., 2013. Compact autonomous voltammetric sensor for sulfide monitoring in deep sea vent habitats. Deep. Sea Res. Part Ocean. Res. Pap. 80, 47–57.

Crenshaw, M.A., Neff, J.M., 1969. Decalcification at the mantle-shell interface in molluscs. Am. Zool. 9 (3), 881–885.

Crone, T.J., Wilcock, W.S.D., 2005. Modeling the effects of tidal loading on mid-ocean ridge hydrothermal systems. Geochem. Geophys. Geosyst. 6; http://dx.doi.org/10.1029/2004GC000905

Eckelbarger, K.J., 1994. Diversity of metazoan ovaries and vitellogenic mechanisms: implication for the life history theory. Proc. Biol. Soc. Wash. 107 (1), 193–218.

Fisher, C.R., 1990. Chemoautotrophic and methanotrophic symbioses in marine invertebrates. Rev. Aquat. Sci. 2, 399–613.

Fornari, D.J., Von Damm, K.L., Bryce, J.G., Cowen, J.P., Ferrini, V., Fundis, A., Lilley, M. D., Luther, G.W., Mullineaux, L.S., Perfit, M.R., Meana-Prado, M.F., Rubin, K.H., Seyfried, W.E., Shank, T.M., Soule, S.A., Tolstoy, M., White, S.M., 2012. The East Pacific Rise between 9°N and 10°N: 25 years of integrated, multidisciplinary oceanic spreading center studies. Oceanography 25 (1), 18–43.

Ghil, M., Allen, R.M., Dettinger, M.D., Ide, K., Kondrashov, D., Mann, M.E., Robertson, A., Saunders, A., Tian, Y., Varadi, F., Yiou, P., 2002. Advanced spectral methods for climatic time series. Rev. Geophys. 40 (1), 3.1–3.41.

Ip, Y.K., Loong, A.M., Kiong, K.C., Wong, W.P., Chew, S.F., Reddy, K., Sivalonganathan, B., Ballantyne, J.S., 2006. Light induces an increase in the pH of and a decrease in the ammonia concentration in the extrapallial fluid of the giant clam Tridacna squamosa. Physiol. Biochem. Zool. 79, 656–664.

Johnson, K.S., Childress, J.J., Beehler, C.L., Sakamoto, C.M., 1994. Biogeochemistry of hydrothermal vent mussel communities: the deep-sea analogue to the intertidal zone. Deep-Sea Res. Part I Ocean Res. Pap. 41 (7), 993–1011.

Kochevar, R., Childress, J.J., Fishrer, C.R., Minnich, L., 1992. The methane mussel: roles of symbiont and host in the metabolic utilization of methane. Mar. Biol. 112, 389–401.

Le Bris, N., Sarradin, P.M, Pennec, S., 2001. A new deep-sea probe for in situ pH measurement in the environment of hydrothermal vent biological communities. Deep Sea Res. Part I 48, 1941–1951.

Le Bris, N., Sarradin, P.M., Caprais, J.C., 2003. Contrasted sulphide chemistries in the environment of 13°N EPR vent fauna. Deep-Sea. Res. I 50, 737–747.

Le Bris, N., Govenar, B., Le Gall, C., Fisher, C.R., 2006. Variability of physico-chemical conditions in 9°50'N EPR diffuse flow vent habitats. Mar. Chem. 98, 167–182.

Le Bris, N., Contreira-Pereira, L., Yücel, M., 2012. In situ chemical sensors for benthic marine ecosystem studies in sensors for ecology. In: Le Galliard, J.-F., Guarini, J.-M., Gaill, F. (Eds.), Towards Integrated knowledge of Ecosystems. CNRS Editions, Paris, France, pp. PP185–208.

Lenihan, H.S., Mills, S.W., Mullineaux, L.S., Peterson, C.H., Fisher, C.R., Micheli, F., 2008. Biotic interactions at hydrothermal vents: Recruitment inhibition by the mussel Bathymodiolus thermophilus. Deep-Sea Res. I 55, 1707–1717.

Liang, X., Thurnherr, A.M., 2012. Eddy-modulated internal waves and mixing on a midocean ridge. J. Phys. Ocean. 42, 1242–1248.

Luther III, G.W., Reimers, C.E., Nuzzio, D.B., Lovalvo, D., 1999. In situ deployment of voltammetric, potentiometric, and amperometric microelectrodes from a ROV to determine O_2, Mn, Fe, S(-2), and pH in porewaters. Environ. Sci. Technol. 33, 4352–4356.

Lutz, R.A., Fritz, L.W., Cerrato, R.M., 1988. A comparison of bivalve (Calyptogena magnifica) growth at two deep-sea hydrothermal vents in the eastern Pacific. Deep-Sea Res. 35 (10/11), 1793–1810.

McGillicuddy, DJ, Lavelle Jr., W, Thurnherr, AM, Kosnyrev, V.K., Mullineaux, L.S., 2010. Larval dispersion along an axially symmetric mid-ocean ridge. Deep. Sea Res. I 57, 880–892.

McConnaughey, T.A., Gillikin, D.P., 2008. Carbon isotopes in mollusk shell carbonates. Geo -Mar. Lett. 28, 287–299.

Moore, T.S., Shank, T.M., Nuzzio, D.B., Luther, G.W., 2009. Time-series chemical and temperature habitat characterization of diffuse flow hydrothermal sites at 9°50'N East Pacific Rise. Deep-Sea Res. II 56, 1616–1621.

Mullineaux, L.S., Le Bris, N., Mills, S.W., Henri, P., Bayer, S.R., Secrist, R.G., Siu, N., 2012. Detecting the influence of initial pioneers on succession at deep-sea vents. PLOS One 7 (12), 1–14.

Nedoncelle, K., Lartaud, F., De Rafelis, M., Boulila, S., Le Bris, N., 2013. A new method for high-resolution bivalve growth rate studies in hydrothermal environments. Mar. Biol. 160 (6), 1427–1439.

Nees, H.A., Lutz, R.A., Shank, T.M., LutherIIIa, G.W., 2009. Pre-and post-eruption diffuse flow variability among tubeworm habitats at 9°50' north on the East Pacific Rise. Deep-Sea Res. Part. II 56, 1607–1615.

Pruis, M.J., Johnson, H.P., 2004. Tapping into the sub-seafloor: examining diffuse flow and temperature from an active seamount on the Juan de Fuca Ridge. Earth Planet. Sci. Lett. 217, 379–388.

Sarrazin, J., Cuvelier, D., Peton, L., Legendre, P., Sarradin, P.M., 2014. High-resolution dynamics of a deep-sea hydrothermal mussel assemblage monitored by the EMSO-Açores MoMAR observatory. Deep. Sea Res. Part I. 90, 62–75.

Scheirer, D.S., Shank, T.M., Fornari, D.J., 2006. Temperature variations at diffuse and focused flow hydrothermal vent sites along the northern East Pacific Rise. Geochem. Geophys. Geosyst. 7, 1–23.

Schöne, B.R., Giere, O., 2005. Growth increments and stable isotope variation in shells of the deep-sea hydrothermal vent bivalve mollusk Bathymodiolus brevior from the North Fiji Basin, Pacific Ocean. Deep-Sea Res. Part I 52, 1896–1910.

Shank, T.M., Fornari, D.J., Von Damm, K.L., Lilley, M.D., Haymon, R.M., Lutz, R.A., 1998. Temporal and spatial patterns of biological community development at nascent deep-sea hydrothermal vents (9°50'N, East Pacific Ris. Deep-Sea Res. Part II 45, 465–515.

Soule, S.A., Fornari, D.J., Perfit, M.R., Rubin, K.H., 2007. New insights into mid-ocean ridge volcanic processes from the 2005-06 eruption of the East Pacific Rise, 9° 46'–56'N. Geology 35, 1079–1082.

Thomson, D.J., 1982. Spectrum estimation and harmonic analysis. Proc. IEEE 70 (9), 1055–1096.

Thurnherr, A.M., Ledwell, J.R., Lavelle, W., Mullineaux, L.S., 2011. Hydrography and circulation near the crest of the East Pacific Rise between 9° and 10°N. Deep. Sea Res. Part I 58, 365–376.

Tunnicliffe, V., Davies, K.T.A., Butterfield, D.A., Embley, R.W., Rose, J.M., Chadwick, W.W., 2009. Survival of mussels in extremely acidic waters on a submarine volcano. Nat. Geosci. 2, 344–348.

Van Dover, C.L., 2000. The Ecology of Deep-Sea Hydrothermal Vents. Princeton, New Jersey.

Van Dover, C.L., 2002. Community structure of mussel beds at deep-sea hydrothermal vents. Mar. Ecol. Prog. Ser. 230, 137–158.

Van Duren, L.A., Herman, P.M.J., Sandee, A.J.J., Heip, C.H.R., 2006. Effects of mussel filtering activity on boundary layer structure. J. Sea Res. 55, 3–14. http://dx.doi.org/10.1016/j.seares.2005.08.001.

Zhang, J.Z., Millero, F.J., 1994. Kinetics of oxidation of hydrogen sulfide in natural waters. In: Alpers, C.N., Blowes, D.W. (Eds.), Environmental Geochemistry of Hydrogen Sulfide in Natural Waters. ACS, Washington DC, pp. 393–411.